Hindawi
Wireless Communications and Mobile Computing
Volume 2022, Article ID 7449392, 9 pages
https://doi.org/10.1155/2022/7449392

Research Article

Dynamic Modelling and Calculation of Crank Slider Mechanism of Multiparameter Friction Model in Wireless Communication

Qian Jing

College of Mechanical Engineering, Long Dong University, Qingyang 745000, Gansu, China

Correspondence should be addressed to Qian Jing; jingq@ldxy.edu.cn

Received 28 December 2021; Accepted 31 January 2022; Published 28 February 2022

Academic Editor: Deepak Kumar Jain

In this research work, an advanced wireless communication-based crank slider mechanism for multiparameter friction techniques is analyzed. The earlier models are unable to find exact friction; therefore, a correct crank function cannot be identified. The dynamic crank sliding mechanism is required for advanced mechanical applications. The available models are not suitable for future mechanical exhibiting. In this work, an SVM-based crank slider with a dynamic friction model is implemented. The SVM mathematical technique continually balances dynamic modeling with friction balancing. Finally, the controller/observer methods showed effective numerical outcomes. The variables of the system are analyzed, noting the mistakes and the estimations that are made. The performance measures accuracy of 98.45%, sensitivity of 97.34%, crank slider of 96.34%, and recall at 97.34%.

1. Introduction

Based on an adaptive self-recursive wavelet neural network (SRWNN) and a sliding mode controller/observer, the slider-crank mechanism may now be controlled in a novel way [1]. As a goal, it is hoped that tracking errors will be reduced. The movement of this device is in relation to a predetermined path. The instigator design is a two-step process. One is a sliding mode approach, while the other is a nonsliding mode strategy. Another component of the controller is an adaptive SRWNN. In this controller mode, the SRWNN weights are first taught offline and then updated online. This is known as adaptive control. Additionally, this research proposes the use of a hybrid control method. The usage of velocity sensors has been phased out in favor of the velocity observer. The research starts followed by the development of the slider-crank mechanism dynamic equations, the recommended observer, and control techniques.

In mechanical transmission, the slider-crank mechanism is a common transmission mechanism. It is difficult to analyze the motion of mechanisms, so we were unable to get performance after we had completed the design and verified it. The slider-crank is a device used in a variety of industries and sectors, such as gasoline and diesel engines, to change a force's linear displacement into a circular movement; otherwise, the other way around. Even if certain conventional methodologies are employed in the literature, this study's major goal is to enhance the previously described studies. Wavelet neural networks have been used in a variety of applications, as is well known. Consideration of various control techniques is offered in this study. A sliding mode controller (SMC) and SRWNN will be used to stabilize this mechanical system, according to the primary goal of this research. The closed-chain mechanical system of the slider-crank is considered.

An observer that does not need sensors to predict velocities is provided in this study. A sliding mode controller and an adaptive self-recurrent wavelet neural network are recommended for the slider-crank mechanism. Other neural network controller strategies have been demonstrated to be inferior to sliding mode control too a self-recurrent wavelet network. Following the separation principle, it is possible to build the observer and controller independently. The self-recurrent wavelet neural network controller is more efficient than existing systems for regulating neural network networks because it has an input layer, a mother wavelet layer, a product layer, and an output layer. The motivation of the paper is to analyze an advanced wireless communication-based crank slider mechanism for multiparameter friction techniques.

2. Literature Survey

According to Azar et al., the numerical experimentation results show that the descending mode and SRWNN controllers provide the minimum tracking error for linear and angular displacements compared to other techniques discovered in the literature [2].

Grigorescu et al. found that the slider-crank base mechanism is employed to operate another gearing linkage chain with linear actuators in this investigation, as shown in the figure. It is feasible to achieve a broad range of rotation angles and transmission angles with this design because of the linear actuator and geared linkage. First-order singularities are avoided using these features and involuntary movement of the closest component to the movable platforms [3].

Lupuţi et al. state that, incorporating a slider-crank mechanism as the foundation, the planar parallel manipulator is operated by a gear linkage with linear actuation and is shown in this paper. Using the slider-geared crank's linear actuators, the article illustrates the actuator strokes of the slider-linear crank. Mobile platform rotation is also factored into two different situations [4].

Huang's findings describe an electric power transmission line robot that may be used to remove bird's nests while the electricians are doing their job. In order to avoid the risk of operating the electricity line in a dangerous manner, this procedure is safe, quick, and efficient [5].

Singh et al. state that by using wearable sensors, this research proposes an innovative and cost-effective method for determining the gait cycle in a variety of locomotor activities. Using a force sensing resistor (FSR), a wireless knee angle monitoring device was built. Both the slider-crank assembly and the wireless signal processing unit are part of the knee angle measuring system. The four-bar slider-crank mechanism is adopted to transform circular motion into reciprocating linear motion by sensing the force provided while walking. The knee angle is monitored live to calculate joint angles in real time at the signal processing unit. Using this method, the knee angle may be measured in a simple and efficient manner [6].

Yan et al. utilized a cooperative working mechanism system with several manipulators and six degrees of freedom to construct a high-performance live working end for insulation wire slicing, clamping, tightening, and loosening. Power distribution detached and linked streamlining robots may efficiently replace the human job and boost system intelligence [7].

All four sections of the robot are included inside this body: an electrically moveable insulating platform, the robot's body, and the working end. At the completion of the process, there are two ends: a wire stripping end and a clip attaching end. Using a robot to charge and detach cables has been shown to be a cost-effective and time-saving alternative to the traditional process [8].

According to Fan et al., to date, this is the first research to describe an entirely new kind of energy harvester rotor: one that is hung and actuated by only two thin threads. Instead of converting mechanical motion into high-resonant-frequency oscillator vibrations, the harvester may convert vibrations or linear reciprocating movements into either rapid rotation or high-frequency small-twisting vibrations of a rotor [9].

Patra states that instead of attempting to directly match the foot trajectory, here we sought to match several geometric features of the region encircled by the foot trajectory. Using the connection's dimensions, neural networks are trained to predict the geometric aspects of the linkage as outputs. The "best-fit dimensions" for the intended trajectory were predicted using the same trained network [10].

According to an experimental investigation by Ternytskyi et al., the torque value is impacted by the rotating speed of a driving shaft in the pressure plate mechanism. This article demonstrates that a screw-nut transmission system may be used to drive a movable pressure plate [11].

Chen and Yao state that the analysis simulation of mechanisms may be carried out easily and the complexity of analysis reduced by utilizing MATLAB analysis simulation software that has powerful functions. It is possible to increase the degree of design efficiency and reduce design expenses [12].

Yu and Wei improved modular slider-crank flapping system that fully utilizes the DC motor's continuous high-speed rotation is suggested and implemented to increase swimming speed. Accordingly, a dolphin robot built using the suggested mechanisms attained great propelling speeds, proving the design's viability [13].

As a result of Wei and Yu's research, a novel flapping mechanism based on slider-cranks and the continuous rotation of a DC motor has been developed. A prototype robot has been developed to assess the efficacy of the design ideas that have been established [14].

Using dynamic analysis, Chang et al. identified where the mechanical switch for the clutch trigger mechanism should be located, and the results were validated by simulation and testing. Future research should focus on creating a two-degree-of-freedom legged locomotion system with an impact slider-crank mechanism and an extra swing actuation [15].

From the studies of Rosen et al., for future revisions, the vehicle's testing sets and the real car have built a strong development environment. By using onboard sensors and an external motion capture arena, the vehicle flew successfully and demonstrated that this platform is suited for insect-scale flight energetic and control studies [16].

Saike and Jiangtao state that the slider's acceleration and the link's angle acceleration may be lowered by raising the link's set over and link length. Based on the simulation results, the best design proposal was chosen from the others. MSGC may minimize the amount of time and effort required to analyze data while increasing the accuracy and efficiency of the process [17].

An examination conducted by Cai et al. on the structural characteristics and the sliding movements within a dual-crank-slider mechanism, as well as the implications of doing so in a cable crawling robot, is presented in this paper, which concludes a useful investigation into the possibility of using the reverse mechanism of a dual-crank-slider mechanism in a cable crawling robot. When attempting to solve the synthesis issue of selecting cable high-altitude walking robot linkage, it has a particular reference value [18].

Wang et al. state that patients' safety is a primary consideration in the design of the device, which does not have quick-return features. A remote monitoring system for medical safety is also being developed to guarantee that patients are able to rehabilitate as intended. According to simulation findings and real experimentation, the suggested rehabilitation approach is both efficient and effective [19].

As an alternative to the velocity sensors, Azar et al. propose using a velocity observer instead. The numerical experiment results show that the sliding mode and SRWNN controllers provide the minimum tracking error for linear and angular displacements compared to other techniques discovered in the literature [2].

The findings of De Groote et al. show that a recurrent implementation of the NNAP model outperforms the feed-forward implementation in terms of system state predictions. By removing the neural network from the model, it is possible to get new insights into the dynamics of the system. To achieve precise estimates of the unknown spring force interaction and friction on the slider mechanism, we used this testing method [20].

The number of hops in the communication system is considerably more in the communication system, and most of the traffic connectivity is not optimized in the existing methods. To overcome these limitations, the proposed method is designed.

3. Methodology

In this section, a brief discussion of the crank slider mechanism of the multiparameter friction mechanism is explained. The connection between modules and their cranks is made by the proposed wireless mode. To correlate and transport cranks of the same broadcast, these antennas used multiband cellular network multiplexing (CNM) resources. These wireless modems provide the directional gain that will aid in the creation of a focused surface between both the sender and receiver. The location of this connection, like many others, is determined by the chip parameters, the number of brief and medium links, and the cracks decision. The goal of putting wireless networks in place is to reduce the number of hops in the communication system and optimize traffic connectivity between the surfaces shown in Figure 1.

Support vector machines (SVMs) for a specified collection of points may be quickly identified using an iterative approach. Support vectors are kept in mind as candidates for our algorithm's candidate support vector set [21, 22]. It uses a greedy strategy to include candidates in the candidate set. There are times when we have to prune away points that are already in the candidate set because they prevent us from adding new ones. For faster convergence, we begin with a pair of points from two separate classes. Optimization-based methods are then used to increase or reduce the number of possible support vectors. For the purpose of meeting the KKT restrictions, the algorithm iteratively traverses the data. As a general rule, our technique requires $O(|S|\ 2)$ amount of memory, where $|S|$ is a vector's size. It demonstrates that the method is superior towards other iterative algorithms, such as SMO and the NPA, in terms of performance. Using a range of real-world datasets, we prove our crank detection.

Under AWGN channel conditions, the BLER results of the designed SVC approach and competing systems are analyzed in Figure 1. At the 10–5 BLER point, the suggested SVC methodology outperforms both. The classic PDCCH was replaced with a polar code-based scheme, yielding a gain of more than 4 dB over the original PDCCH and roughly 1.1 dB over the polar code-based technique. Even in real-world scenarios like EPA and EVA circuits in LTE-advanced, the suggested SVC scheme maintains its performance advantage over competing systems:

$$\begin{aligned} y &= HRs + v, \\ x &= Cs = s_1 c_1 + s_3 c_3. \end{aligned} \tag{1}$$

Cracks in pieces are arranged to change horizontal movement to rotational movement, such as in a recurrent petrol engine, or rotational movement to linear direction, such as in a revolving piston pump:

$$\begin{aligned} C &= \frac{1}{\alpha}\begin{bmatrix} 1 & 1 & 1 & 1 & 1 & -1 & -1 & -1 & -1 & -1 \\ 1 & -1 & 1 & -1 & -1 & 1 & 1 & -1 & -1 & 1 \\ 1 & 1 & -1 & -1 & -1 & 1 & -1 & -1 & 1 & 1 \\ 1 & -1 & -1 & 1 & 1 & 1 & 1 & 1 & -1 & -1 \\ -1 & 1 & 1 & 1 & 1 & -1 & -1 & -1 & 1 & 1 \end{bmatrix}, \\ y &= Hx + v = \left[Hc_1 Hc_3\right]\begin{bmatrix} s_1 \\ s_3 \end{bmatrix} + v, \\ y &= HCs + v \\ &= \begin{bmatrix} h_{11} & & \\ & \ddots & \\ & & h_{mm} \end{bmatrix}\begin{bmatrix} | & & | \\ c_1 & \cdots & c_N \\ | & & | \end{bmatrix}\begin{bmatrix} s_1 \\ \vdots \\ s_N \end{bmatrix} + \begin{bmatrix} v_1 \\ \vdots \\ v_N \end{bmatrix}, \\ r_{svc} &= \frac{b_i}{2m} = \frac{1}{3(1+\beta)} < \frac{1}{3} = r_{p\ dc\ ch}, \\ &= \tilde{H}Cs + \tilde{v}, \\ w_j &= \arg\max_l \left|\langle \varnothing_1, r^{j-1}\rangle\right|^2, \\ S^* &= \arg\max_{\|s\|_0 = K} P_r\left(\tilde{y}|S, \tilde{H}, C\right), \\ \Omega_s^* &= \arg\max_{|\Omega_s| = K} P_r\left(\tilde{y}|\Omega_s, \tilde{H}, C\right), \\ f_{\|h\|_2^2}(x) &= \frac{x^{m-1}\exp(-x)}{\Gamma(m)}, \\ f_{2\|h\|_2^2}(x) &= \frac{x^{m-1}\exp(-x/2)}{2^m\Gamma(m)}, \\ f_{h_2^2}(x) &= \frac{x^{m-1}\exp(-x)}{\Gamma(m)}, \\ P_{\text{succ}} &= P\left(\Omega_s^* = \Omega_s\right) = P\left(S^1, S^2\right) \\ &= P\left(S^2 \mid S^1\right) P\left(S^1\right). \end{aligned} \tag{2}$$

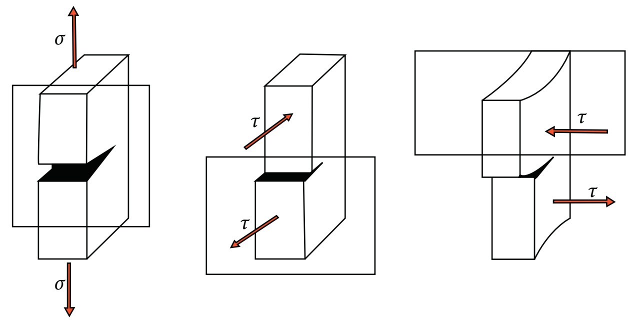

Figure 1: Crank detection.

A 4 system with 3 movable joints and a pyramidal, or gliding, junction is known as a sliding connection. The continuous motion of the sliders is driven by the revolution of the cranks, or the spinning of the rotary motion might be driven by the contraction of gases against a moving piston. Inline and offsets sliders crank are the 2 categories of slider cranks.

Inline: the sliders on the in-toggle are placed such that the direction of movement of the movable junction of the sliders goes through the crank's base joint. As the crank turns, the symmetrical slider motion of back and forth is created.

The slider's motion is not symmetric if the line of motion of the pivoted joint of the adjuster does not really travel through the bottom pivoting of the cranks. In one direction, it goes quicker than in the opposite, which is called the fast technique:

$$P_{\text{succ}} \geq \left(1-\left(1+\frac{(1-\mu^*)^2}{\sigma_v^2}\right)^{-m}-\left(1+\frac{1}{\sigma_v^2}\right)\right)^{2N},$$

$$P_{\text{succ}} \gtrsim \left(1-\left(1+\frac{(1-\mu^*)^2}{\sigma_v^2}\right)^{-m}\right)^{2N},$$

$$\text{BLER}_{\text{svc}} \lesssim 1-\left(1-\left(1+\frac{(1-\mu^*)^2}{\sigma_v^2}\right)^{-m}\right)^{2N},$$

$$P\left(S^1\right) \geq \left(1-\left(1+\frac{(1-\mu^*)^2}{\sigma_v^2}\right)^{-m}-\left(1+\frac{1}{\sigma_v^2}\right)^{-m}\right)^{N-1}. \tag{3}$$

The accompanying diagram, which has the moving parts lightly colored, better depicts the core structure of the mechanism and the relative movement of the pieces. Part 1, the pump's or engine's immovable frame or block, contains a cylinder in which the pistons, part 4, glide back and forth, as seen in the cross-sectional area by the sidewalls DE and FG. The small circle at A represents the main propeller bearing, which is also in part 1. Part 2 of the crank is shown as a single component that connects the central shaft at A to the pulley bearings at B and hence to part 3 of the driving shaft. The bracket is illustrated as a linear element that runs from the piston pin bearing at B to the wrist pin bearings at C, connecting it to the engine, which is portrayed in part 4 as a rectangle. The three bearings at A, B, and C, shown as circles, enable the coupled parts to freely rotate with respect to one another. When B is at point h, the piston will be in position H, and when B is at point j, the piston will be in position J. The face end of the canister (where the gas mixtures explode) is at EG on a petrol engine; the stress caused through the outburst will push the piston as of position H to position J; and the potential motion of a piston connected to the crankshaft and rotating around a load-carrying intercalated with carrying A will be required to return movement from J to H. A generator would have driven the shaft of a mechanical pumping mechanism.

When used in conjunction with a rotating shaft, it produces a reciprocating straight-line motion that is similar to that of a slider-crank mechanism. It is especially effective when the reciprocating motion's needed stroke is modest in contrast to the driving shaft's dimensions. The eccentric disc 2 has an eccentricity AB and is fastened off center to the rotational shaft at A in the illustration. The strap and rod 3 are made up of two sections that are secured together and slide into a groove on the disk's perimeter. Within housing 1, the rod is attached to piston 4. The eccentric slips within the strap as the shaft rotates, and piston 4 travels in a straight path of length 2AB. In a slider-crank system, AB represents the crankshaft and BC represents the connecting rod. Because an eccentric may be mounted anywhere along a shaft, no section of the shaft has to be turned into a crank. Eccentrics are widely employed to drive the valve gears of engines and are seldom utilized to convey huge forces due to excessive friction loss, as shown in Figure 2.

Searching for algorithms that use externally given examples to build generalizations is the goal of supervised machine learning (SML) theorems, which are then used to forecast the future. Figure 3 shows the load moment. Machine learning (ML) categorization under supervision comparisons of different supervised learning is determined by the most efficient algorithm. The data collection is used to determine the categorization algorithm variables and the number of occurrences (features). Seven different techniques for machine learning were used: Random Forest (RF),

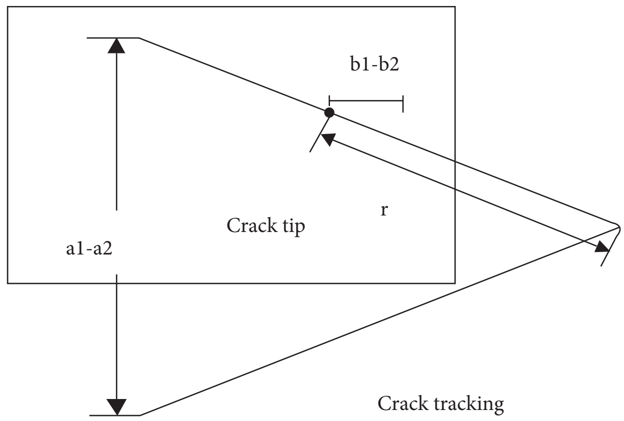

Figure 2: Crack tracking.

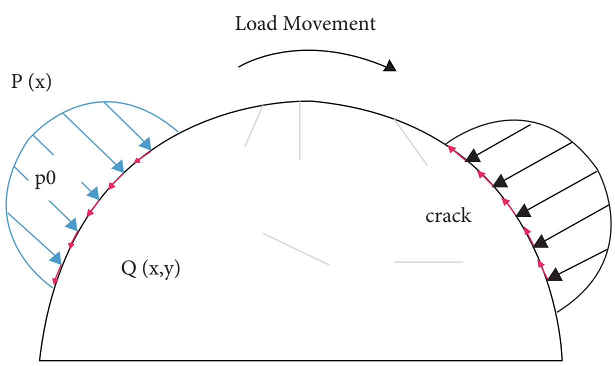

Figure 3: Load moment.

Decision Tables (DT), Support Vector Machine (SVM), Naive Bayes (NB), JRip and Decision (j48), and Neural Networks (NN Perception).

In the realm of machine learning (ML) and pattern categorization, SVMs have lately acquired importance. Creating a linear or nonlinear separation surface in the input space is a key step in the classification process. The separating function in support vector classification may be written as the linear combination of kernels associated with each support vectors.

$$f(x) = \sum_{x_j \in S} \propto_j y_j \left(x_j, x\right) + b, \tag{4}$$

where xi is the number of training patterns, $yi \in \{+1, 1\}$ is the number of related class labels, and S is the number of support vectors.

Resulting from the combination of the two formulations,

$$\min_{0 \le \propto_{i \le C}} W = \frac{1}{2} \sum_{I,J} \propto_i Q_{ij} \propto_j - \sum_i \propto_i + b \sum_i y_i, \tag{5}$$

where $\propto_i$ are the corresponding coefficients, b is the offset, $Q_{ij} = y_i y_J K\,(x_i, x_j)$ is a symmetric definite kernel matrix, and C is the parameter used to penalize error point in the separable case. The Karush–Kuhn–Tucker (KKT) conditions for the dual can be expressed as follows.

Here, $\propto_i$ are the coefficients for each corresponding coefficient and the offset, b, for each of the corresponding coefficients. For separable cases, the error points are penalized by $Q_{ij} = y_i y_J K\,(x_i, x_j)$ being a symmetric definite kernel matrix. It is possible to specify the KKT conditions for the dual in terms of KKT.

$$g_i = \frac{\partial w}{\partial \propto_i} = \sum_i Q_{ij} \propto_j + y_i b - 1 = y_i\, f\left(x_i\right) - 1, \tag{6}$$

$$\frac{\partial w}{\partial b} = \sum_j y_j \propto_j = 0. \tag{7}$$

This divides the training set into three parts: S, the support vector set $(0 < \propto_i < C, g_i = 0)$, E, the error set $\propto_i = C, g_i < 0$, and R, the well-classified set $(\propto_i = 0, g_i > 0)$.

For example, if points in error are punished quadratically with C', the issue may be reduced to a separable case with $C = \infty$. According to the Kernel's new design,

$$K'\left(x_i, x_j\right) = K\left(x_i, x_j\right) + \frac{1}{C'} \delta_{ij}, \tag{8}$$

where $\delta_{ij} = 1$ if $I = j$ and $\delta_{ij} = 0$ or else. The SVM issue is reduced to a linearly separable instance as a result of this approach.

Numerical library approaches are used to solve a quadratic optimization issue during the SVM training. This is a computationally costly process that has the potential for instability and is difficult to accomplish. One solution is to use iterative methods such as the sequential minimal optimization (SMO) and the nearest point algorithm (NPA). An additional piece of evidence is presented here.

This method keeps track of a list of possible support vectors. Starting with a pair of points from opposing classes is similar to DirectSVM's strategy. The program does not hesitate to add any infringing points it identifies to the list of possible candidates. It is possible that other support vectors in the set may impede the insertion of the violating point as a support vector. We remove all of these points from the candidate set by deleting them. In order to make sure that the KKT requirements are met, we go over the dataset again until no violations are discovered. The

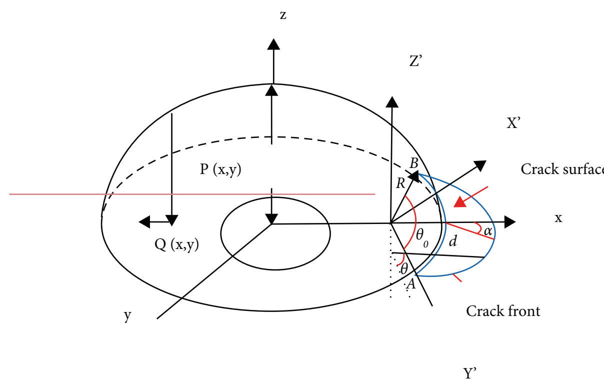

FIGURE 4: Crack surface tracking.

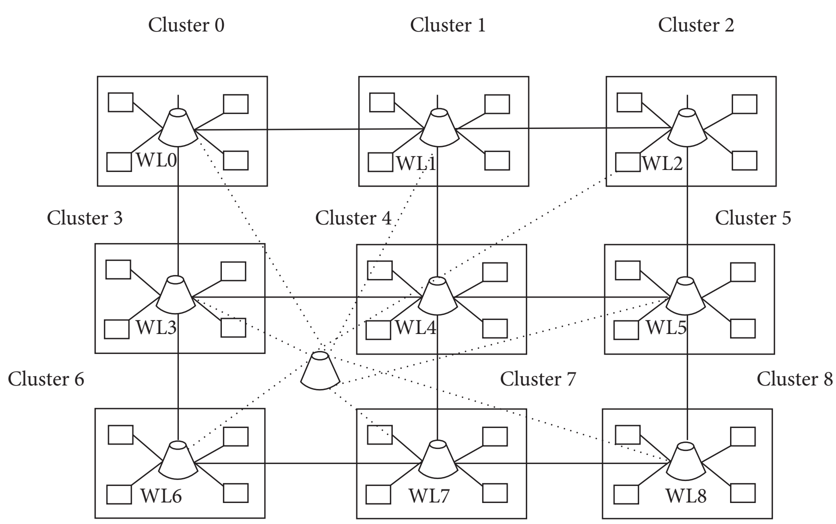

FIGURE 5: Establishing a wireless link between cores.

TABLE 1: Comparison of results.

Metrics/methods		GA [70]	Xboosting [77]	RFO [77]	FCNN [73]	Proposed
Theory	*Accuracy*	77.775	77.773	87.867	83.076	88.665
	Precision	78.85	78.37	87.57	85.07	88.667
	Recall	57.378	57.756	77.805	87.665	88.355
	F7 score	53.56	58.765	77.85	83.765	88.665
Simulation results	*Accuracy*	73.77	77.76	85.85	85.77	88.667
	Sensitivity	73.86	77.35	85.56	87.08	88.663
	Specificity	57.37	58.757	77.87	87.667	88.355
	F7 score	58.57	60.767	77.83	86.765	88.663

quadratic penalty formulation is used to verify that the data points in the kernel space are linearly separable, as shown in Figure 4.

4. Results and Discussion

In these sections, a brief discussion of wireless communication-based crank detection is performed through the proposed SVM model. Figure 5 clearly explains about wireless communication protocol-based crank detection system. The surface is tracked with point A and near end 2–1/4 crankshaft is adjusting. The holes and crank connections are pivoting slider with punch (Table 1).

The above theory-based crank analysis-based wireless communication model is shown in Figure 6.

The containers can also be drained whenever the depth or vacant space calculated by the wireless sensor exceeds the threshold level. The time interval for emptying the bins is set to 8 hours, and the bins can also be emptied whenever the depth or vacant space calculated by the ultrasonic sensor

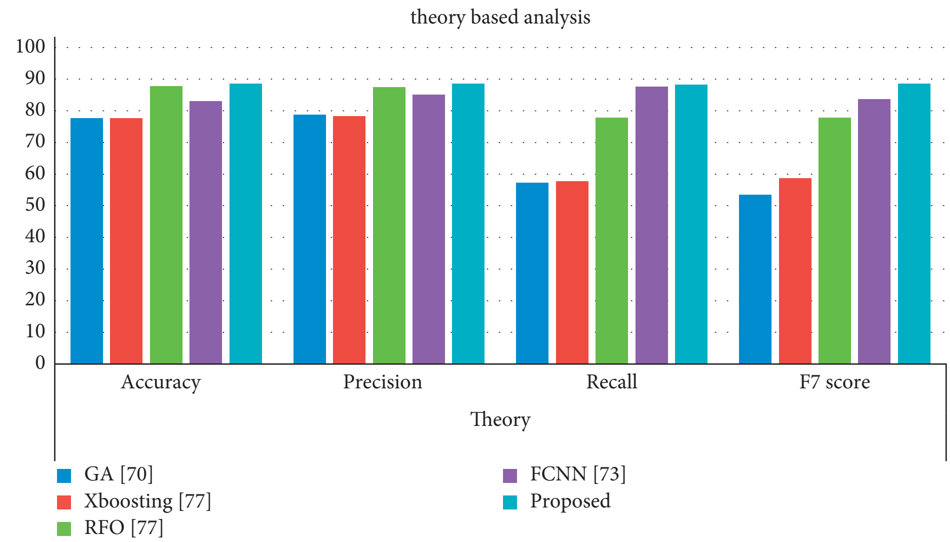

Figure 6: Theory-based crank analysis.

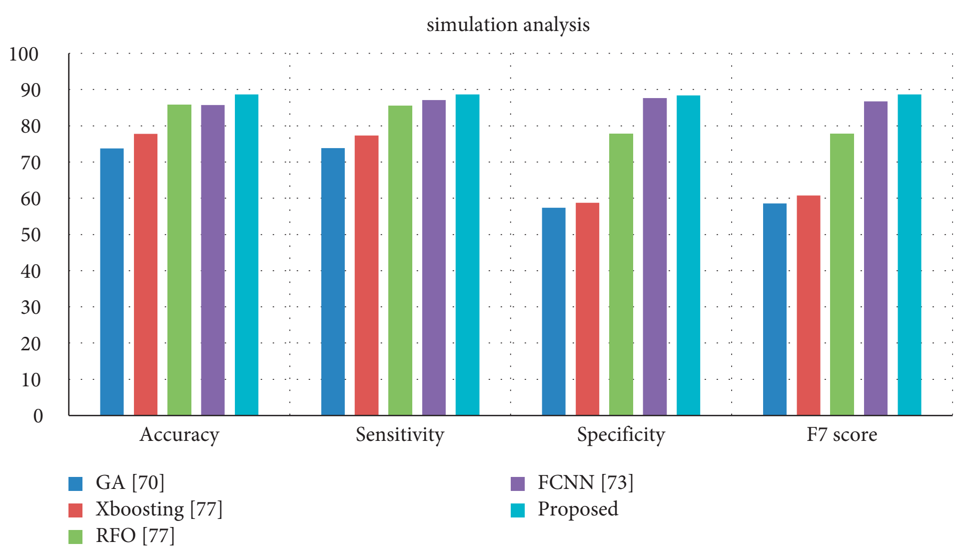

Figure 7: Simulation based crank analysis.

reaches the specified level. To assess and understand the frequency and interval at which the data gathering is optimum, the information is shown with time versus depth of the cranks, as shown in Figure 7.

As observed from Figure 8, the default depth of the crank is 35 nm. Whenever the bin is emptied, the ultrasonic sensor reads a value of 35. Each bar in this graph represents the vacant space available in that hour. Whenever the value is less than our threshold value of 5, the user is alerted to clear the bin. So, the depth in the next hour is a value of 35.

The following are input images along with their outputs. The object in the input image is a waste object that is classified by our classification model, and the result can be observed in the output terminal of the python IDE. The output is either “Dry” or “Wet” based on the classification of the input image.

The crank area was the emphasis of this research, as well as its implementation on numerous hardware devices. It also discussed the numerous steps accomplished in this sector as well as its possible uses. It may be able to come up with some

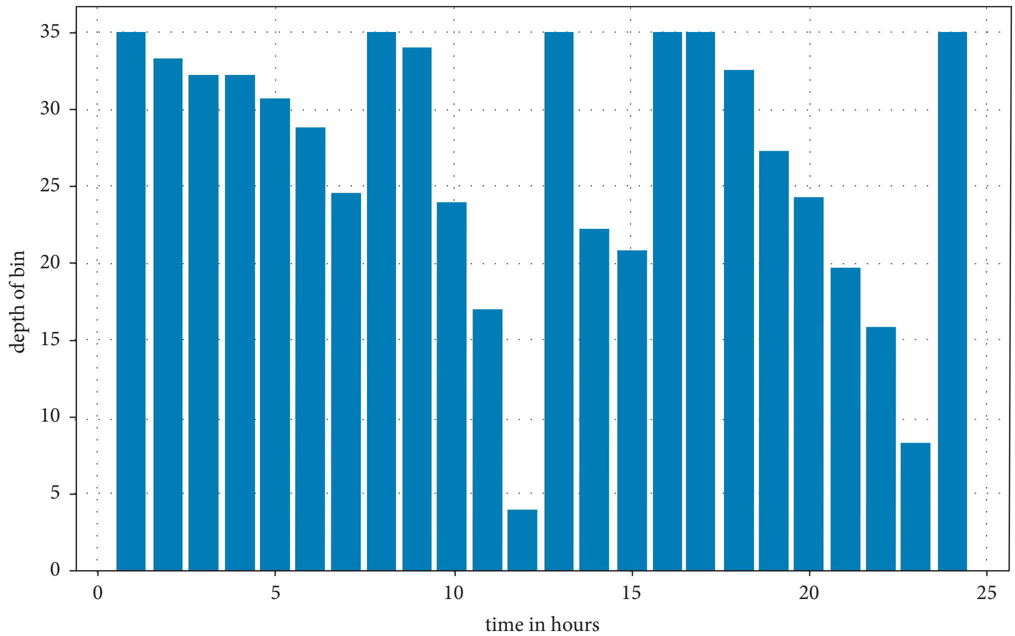

Figure 8: Time vs depth of the crank.

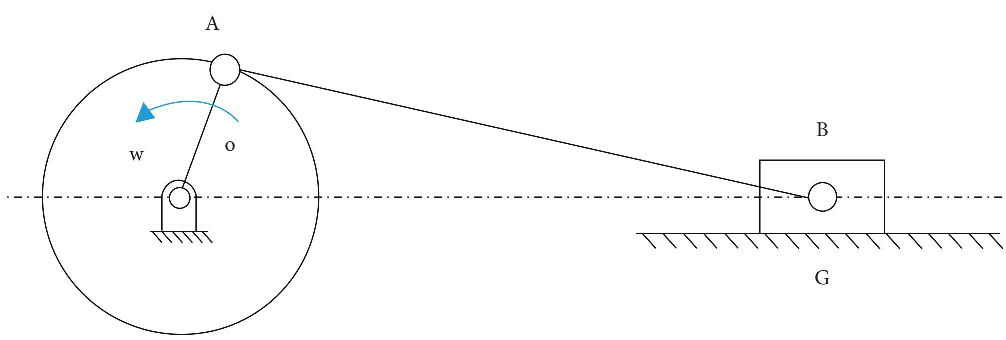

Figure 9: Crank detection.

novel picture security concepts in the next few years, as shown in Figure 9.

5. Conclusion

An innovative wireless communication-based crank slider mechanism for multiparameter friction approaches is investigated in this study. Since older versions could not discover accurate friction, the right crank function could not be determined. For sophisticated mechanical applications, the dynamic crank sliding mechanism is necessary. The current types are unsuitable for future mechanical displays. An SVM-based crank slider with dynamic friction is developed in this study. Dynamic modeling and friction balancing are constantly balanced using the SVM mathematical approach. Finally, the numerical outputs of the controller/observer approaches are successfully presented. The system's variables are analyzed, noting any errors or assumptions that were made. The performance is rated as follows: 98.45 percent accuracy, 97.34 percent sensitivity, 96.34 percent crank slider, and 97.34 percent recall.

Data Availability

The data that support the findings of this study are available from the corresponding author upon reasonable request.

Conflicts of Interest

The author declares that there are no potential conflicts of interest with this research and publication of this article.

Acknowledgments

This work was supported by the Gansu Natural Science Foundation (No. 21JR7RM190), the Qingyang Natural Science Foundation (No. QY2021A-F008), the Gansu University Innovation Foundation (No. 2021B-277), the

Doctoral Foundation of Longdong University (XYBY1906), and the Gansu Science and Technology (No. 20JR5RA483).

References

[1] H. Chen, Y. Lu, and L. Tu, "Fault identification of gearbox degradation with optimized wavelet neural network," *Shock and Vibration*, vol. 20, no. 2, pp. 247–262, 2013.

[2] A. T. Azar, F. E. Serrano, Q. Zhu, S. Vaidyanathan, and J. M. Rossell, "Adaptive self-recurrent wavelet neural network and sliding mode controller/observer for a slider crank mechanism," *International Journal of Computer Applications in Technology*, vol. 63, no. 4, pp. 273–285, 2020.

[3] S. M. Grigorescu, A.-M.-F. Lupuţi, I. Maniu, and E.-C. Lovasz, "Novel planar parallel manipulator using geared slider-crank with linear actuation as connection kinematic chain," in *Proceedings of the European Conference on Mechanism Science*, pp. 496–505, Springer, Cham, Germany, 2020 September.

[4] A. M. F. Lupuţi, S. M. Grigorescu, E. C. Lovasz, C. Sticlaru, and I. Cărăbaş, "Kinematics of the planar parallel manipulator using geared slider-crank with linear actuation as legs 3-R (PRRGR) RR," in *Proceedings of the Joint International Conference on Mechanisms and Mechanical Transmissions and the International Conference on Robotics*, pp. 249–261, Springer, Cham, Germany, 2020 October.

[5] Z. Huang, "A structural design of a robot for removing bird's nest on power transmission line," in *Proceedings of the 3rd International Conference on Mechatronics Engineering and Information Technology (ICMEIT 2019)*, pp. 172–176, Atlantis Press, Atlantic, NJ, USA, 2019 April.

[6] R. Singh, H. Singh, and A. K. Godiyal, "Wearable knee joint angle measurement system based on force sensitive resistors," in *Proceedings of the 2018 IEEE Long Island Systems, Applications and Technology Conference (LISAT)*, pp. 1–3, IEEE, Farmingdale, NY, USA, 2018 May.

[7] Y. Yan, X. Xu, Z. Xiao, and X. Tong, "Mechanism design of electric robot of distribution network for cut off or connection of leading wire," *IOP Conference Series: Earth and Environmental Science*, vol. 237, no. 6, Article ID 062027, 2019.

[8] Y. Yan, L. Liu, Z. Zhou, and Y. Fan, "Development of live working robot for distribution network," *IOP Conference Series: Earth and Environmental Science*, vol. 237, no. 6, Article ID 062026, 2019.

[9] K. Fan, M. Cai, F. Wang et al., "A string-suspended and driven rotor for efficient ultra-low frequency mechanical energy harvesting," *Energy Conversion and Management*, vol. 198, Article ID 111820, 2019.

[10] S. Patra, "Designing a cross trainer using an artificial neural network," *Computer Assisted Mechanics and Engineering Sciences*, vol. 28, no. 2, pp. 119–138, 2021.

[11] S. Ternytskyi, I. Rehei, N. Kandiak, I. Radikhovskyi, and O. Mlynko, "Experimental research of paperboard cutting in die cutting press with the screw-nut transmission of drive mechanism of a movable pressure plate," *Acta Mechanica et Automatica*, vol. 15, no. 3, pp. 122–131, 2021.

[12] J. P. Chen and Z. H. Yao, "Study on the simulation of slider-crank mechanisms based on MATLAB," *Journal of Anhui Technical Teachers College*, vol. 4, 2005.

[13] J. Yu and C. Wei, "Towards development of a slider-crank centered self-propelled dolphin robot," *Advanced Robotics*, vol. 27, no. 12, pp. 971–977, 2013.

[14] C. Wei and J. Yu, "Mechanical design of a slider-crank centered robotic dolphin," in *Proceedings of the 10th World Congress on Intelligent Control and Automation*, pp. 3741–3746, IEEE, Beijing, China, 2012 July.

[15] D. Chang, J. Kim, D. Choi, K.-J. Cho, T. Seo, and J. Kim, "Design of a slider-crank leg mechanism for mobile hopping robotic platforms," *Journal of Mechanical Science and Technology*, vol. 27, no. 1, pp. 207–214, 2013.

[16] M. H. Rosen, G. le Pivain, R. Sahai, N. T. Jafferis, and R. J. Wood, "Development of a 3.2 g untethered flapping-wing platform for flight energetics and control experiments," in *Proceedings of the 2016 IEEE International Conference on Robotics and Automation (ICRA)*, pp. 3227–3233, IEEE, Stockholm, Sweden, 2016 May.

[17] C. Saike and L. Jiangtao, "Optimal design of crank-slider mechanisms based on simulation of movement," *Journal of Mechanical Transmission*, vol. 6, 2007.

[18] G. C. Cai, X. M. Zhou, and Z. Wang, "Mechanical structure design based on dual-crank-slider mechanism of the cable crawling robot," *Journal of Machine Design*, vol. 11, 2010.

[19] D. Wang, X. Gao, and Y. Liu, "A robotic extremities muscle rehabilitation system for quadriplegia," in *Proceedings of the 2011 IEEE International Conference on Mechatronics and Automation*, pp. 1190–1195, IEEE, Beijing, China, 2011 August.

[20] W. De Groote, E. Kikken, E. Hostens, S. Van Hoecke, and G. Crevecoeur, "Neural network augmented physics models for systems with partially unknown dynamics: application to slider-crank mechanism," 2021, https://arxiv.org/abs/1910.12212.

[21] Z. Wan, Y. Dong, Z. Yu, H. Lv, and Z. Lv, "Semi-supervised support vector machine for digital twins based brain image fusion," *Frontiers in Neuroscience*, vol. 15, Article ID 705323, 2021.

[22] T.-Y. Kim, H. Ko, S.-H. Kim, and H.-D. Kim, "Modeling of recommendation system based on emotional information and collaborative filtering," *Sensors*, vol. 21, no. 6, p. 1997, 2021.